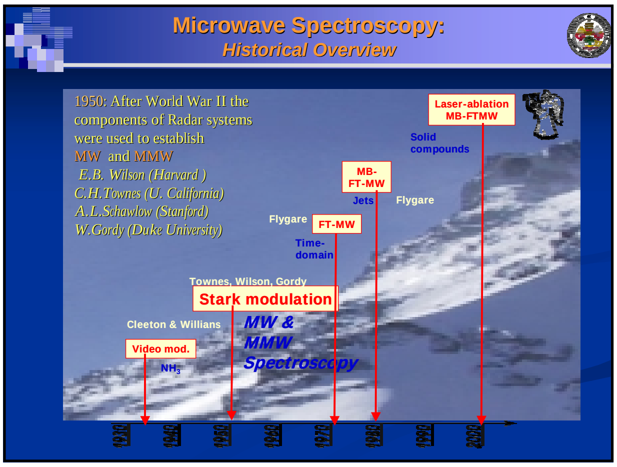

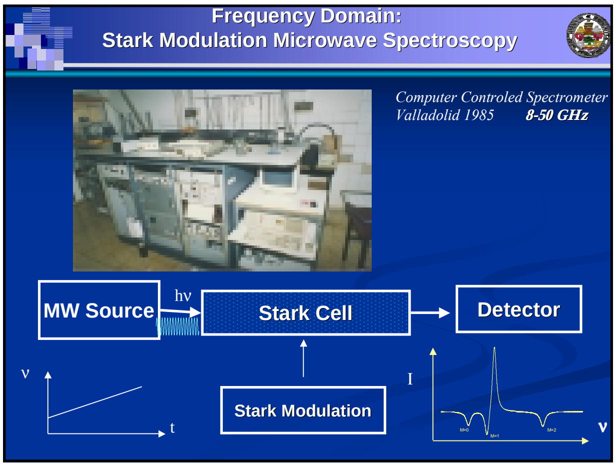

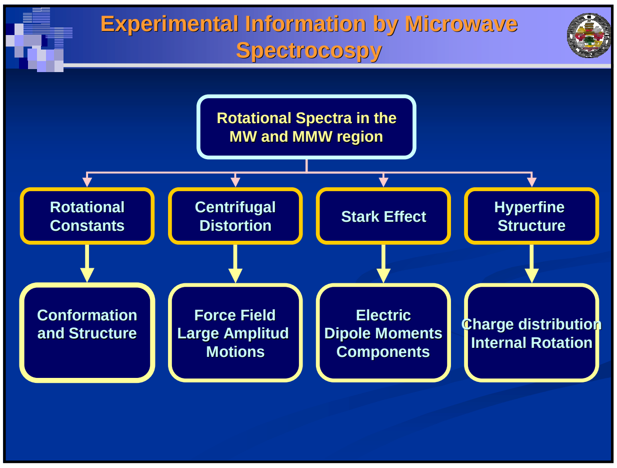

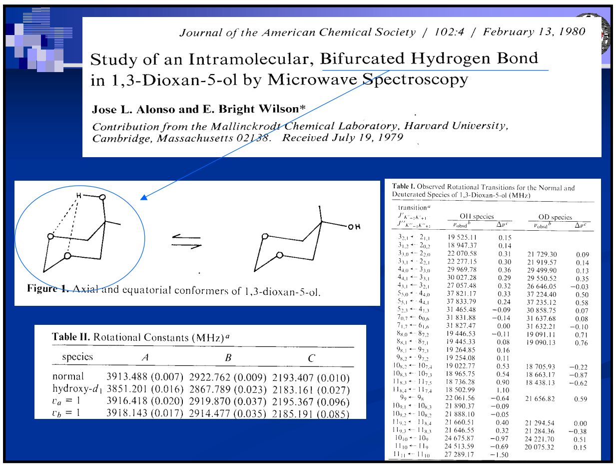

Journal of the American Chemical Society / 102:4 / February 13, 1980

Study of an Intramolecular, Bifurcated Hydrogen Bond in 1,3-Dioxan-5-ol by Microwave Spectroscopy

Jose L. Alonso and E. Bright Wilson*

Contribution from the Mallinckrodt Chemical Laboratory, Harvard University, Cambridge, Massachusetts 02138. Received July 19, 1979

Figure 1. Axial and equatorial conformers of 1,3-dioxan-5-ol.

Table I. Observed Rotational Transitions for the Normal and Deuterated Species of 1,3-Dioxan-5-ol (MHz)

transition[a] $J'_{K'_{-1}K'_{+1}} \leftarrow J''_{K''_{-1}K''_{+1}}$	OH species ν_{obsd}[b]	OH species $\Delta\nu$[c]	OD species ν_{obsd}[b]	OD species $\Delta\nu$[c]
$3_{2,1} \leftarrow 2_{1,1}$	19 525.11	0.15		
$3_{1,2} \leftarrow 2_{0,2}$	18 947.37	0.14		
$3_{3,0} \leftarrow 2_{2,0}$	22 070.58	0.31	21 729.30	0.09
$3_{3,1} \leftarrow 2_{2,1}$	22 277.15	0.30	21 919.57	0.14
$4_{4,0} \leftarrow 3_{3,0}$	29 969.78	0.36	29 499.90	0.13
$4_{4,1} \leftarrow 3_{3,1}$	30 027.28	0.29	29 550.52	0.35
$4_{3,1} \leftarrow 3_{2,1}$	27 057.48	0.32	26 646.05	−0.03
$5_{5,0} \leftarrow 4_{4,0}$	37 821.17	0.33	37 224.40	0.50
$5_{5,1} \leftarrow 4_{4,1}$	37 833.79	0.24	37 235.12	0.58
$5_{2,3} \leftarrow 4_{1,3}$	31 465.48	−0.09	30 858.75	0.07
$7_{0,7} \leftarrow 6_{0,6}$	31 831.88	−0.14	31 637.68	0.08
$7_{1,7} \leftarrow 6_{1,6}$	31 827.47	0.00	31 632.21	−0.10
$8_{8,0} \leftarrow 8_{7,2}$	19 446.53	−0.11	19 091.11	0.71
$8_{8,1} \leftarrow 8_{7,1}$	19 445.33	0.08	19 090.13	0.76
$9_{8,1} \leftarrow 9_{7,3}$	19 264.85	0.16		
$9_{8,2} \leftarrow 9_{7,2}$	19 254.08	0.11		
$10_{8,2} \leftarrow 10_{7,4}$	19 022.77	0.53	18 705.93	−0.22
$10_{8,3} \leftarrow 10_{7,3}$	18 965.75	0.54	18 663.17	−0.87
$11_{8,3} \leftarrow 11_{7,5}$	18 736.28	0.90	18 438.13	−0.62
$11_{8,4} \leftarrow 11_{7,4}$	18 502.99	1.10		
$9_9 \leftarrow 9_8$	22 061.56	−0.64	21 656.82	0.59
$10_{9,1} \leftarrow 10_{8,3}$	21 890.37	−0.09		
$10_{9,2} \leftarrow 10_{8,2}$	21 888.10	−0.05		
$11_{9,2} \leftarrow 11_{8,4}$	21 660.51	0.40	21 294.54	0.00
$11_{9,3} \leftarrow 11_{8,3}$	21 646.55	0.32	21 284.36	−0.38
$10_{10} \leftarrow 10_9$	24 675.87	−0.97	24 221.70	0.51
$11_{10} \leftarrow 11_9$	24 513.59	−0.69	20 075.32	0.15
$11_{11} \leftarrow 11_{10}$	27 289.17	−1.50		

Table II. Rotational Constants (MHz)[a]

species	*A*	*B*	*C*
normal	3913.488 (0.007)	2922.762 (0.009)	2193.407 (0.010)
hydroxy-d_1	3851.201 (0.016)	2867.789 (0.023)	2183.161 (0.027)
$v_a = 1$	3916.418 (0.020)	2919.870 (0.037)	2195.367 (0.096)
$v_b = 1$	3918.143 (0.017)	2914.477 (0.035)	2185.191 (0.085)

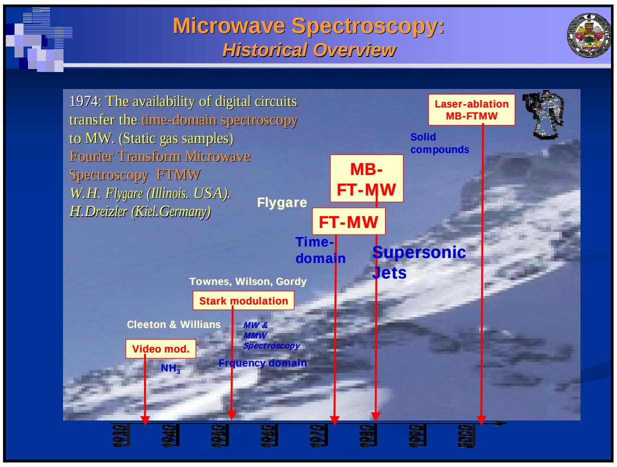
Microwave Spectroscopy:
Historical Overview
1974: The availability of digital circuits transfer the time-domain spectroscopy to MW. (Static gas samples)
Fourier Transform Microwave Spectroscopy FTMW
W.H. Flygare (Illinois. USA).
H.Dreizler (Kiel.Germany)
Laser-ablation MB-FTMW
Solid compounds
MB-FT-MW
Flygare
FT-MW
Time-domain
Supersonic Jets
Townes, Wilson, Gordy
Stark modulation
Cleeton & Willians
Video mod.
MW & MMW Spectroscopy
Frequency domain
NH3

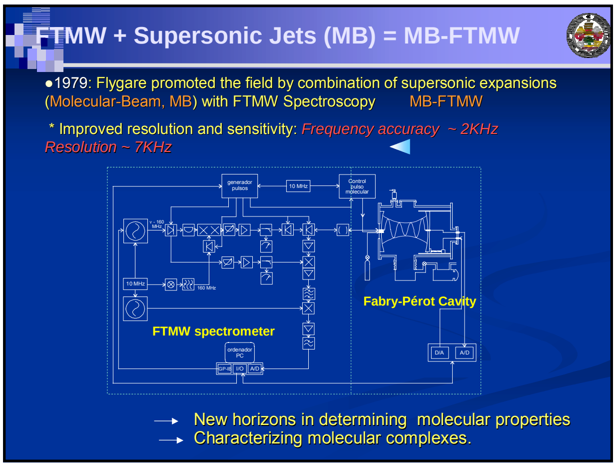
FTMW + Supersonic Jets (MB) = MB-FTMW
●1979: Flygare promoted the field by combination of supersonic expansions (Molecular-Beam, MB) with FTMW Spectroscopy MB-FTMW
* Improved resolution and sensitivity: Frequency accuracy ~ 2KHz
Resolution ~ 7KHz
Fabry-Pérot Cavity
FTMW spectrometer
New horizons in determining molecular properties
Characterizing molecular complexes.

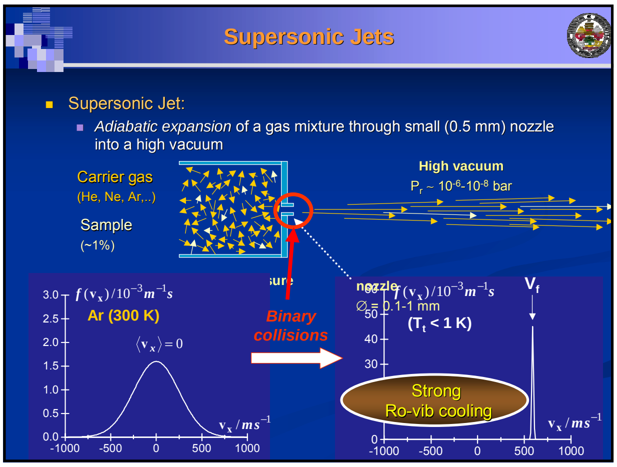
Supersonic Jets
Supersonic Jet:
Adiabatic expansion of a gas mixture through small (0.5 mm) nozzle into a high vacuum
Carrier gas
(He, Ne, Ar,..)
Sample
(~1%)
High vacuum
Pr ~ 10-6-10-8 bar
Ar (300 K)
Binary collisions
nozzle
∅ = 0.1-1 mm
(Tt < 1 K)
Vf
Strong
Ro-vib cooling

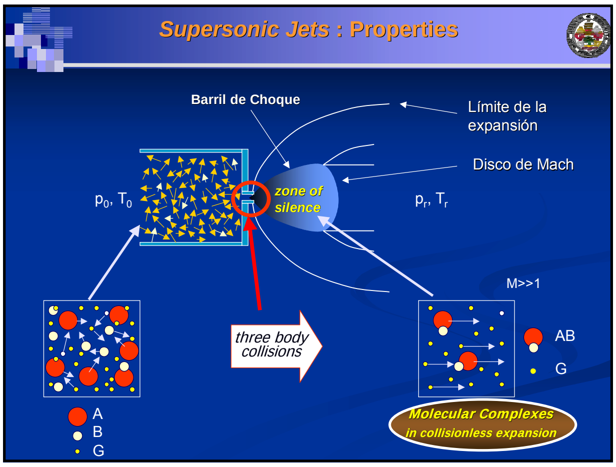
Supersonic Jets : Properties
Barril de Choque
Límite de la expansión
Disco de Mach
p0, T0
zone of silence
pr, Tr
M>>1
three body collisions
A
B
G
AB
G
Molecular Complexes
in collisionless expansion

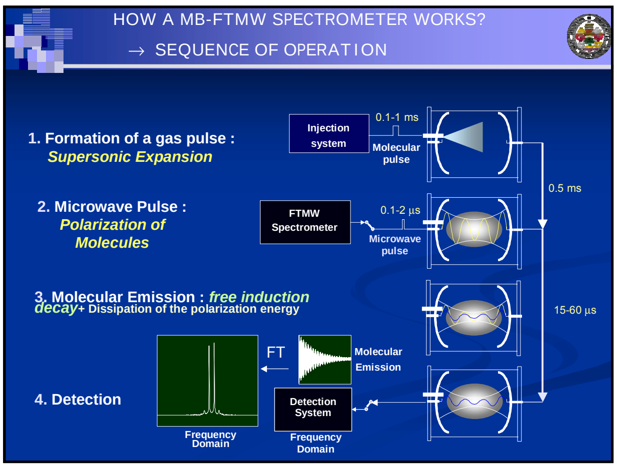
HOW A MB-FTMW SPECTROMETER WORKS?
→ SEQUENCE OF OPERATION
1. Formation of a gas pulse :
Supersonic Expansion
Injection system
0.1-1 ms
Molecular pulse
0.5 ms
2. Microwave Pulse :
Polarization of Molecules
FTMW Spectrometer
0.1-2 µs
Microwave pulse
3. Molecular Emission : free induction decay+ Dissipation of the polarization energy
15-60 µs
FT
Molecular Emission
4. Detection
Detection System
Frequency Domain
Frequency Domain

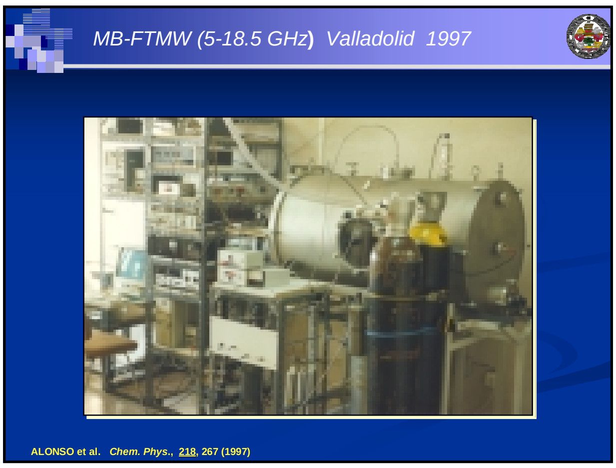
MB-FTMW (5-18.5 GHz) Valladolid 1997
ALONSO et al. Chem. Phys., 218, 267 (1997)

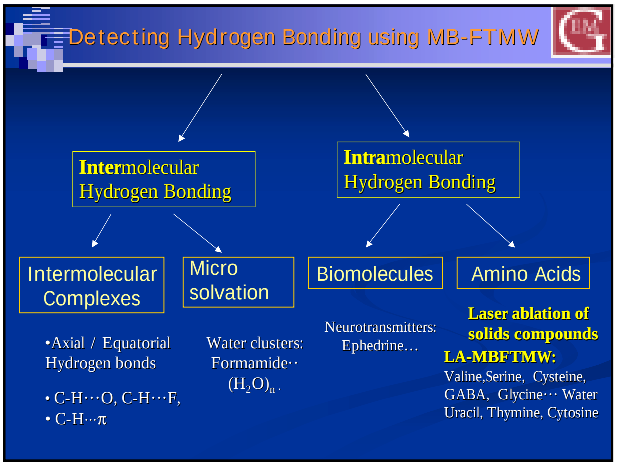
Detecting Hydrogen Bonding using MB-FTMW
Intermolecular Hydrogen Bonding
Intramolecular Hydrogen Bonding
Intermolecular Complexes
Micro solvation
Biomolecules
Amino Acids
•Axial / Equatorial Hydrogen bonds
• C-H···O, C-H···F,
• C-H···π
Water clusters: Formamide··
(H2O)n .
Neurotransmitters: Ephedrine…
Laser ablation of solids compounds
LA-MBFTMW:
Valine,Serine, Cysteine, GABA, Glycine··· Water
Uracil, Thymine, Cytosine

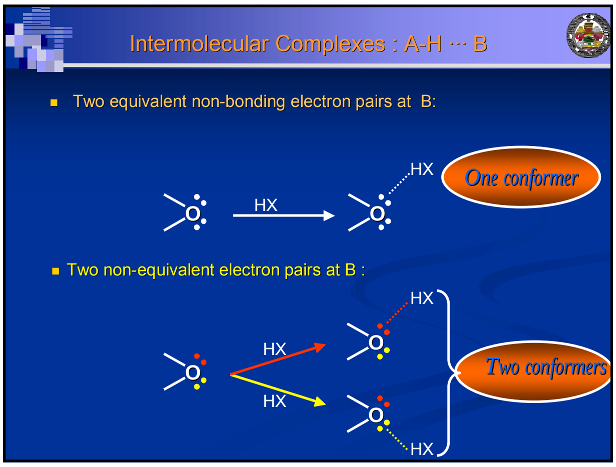
Intermolecular Complexes : A-H ··· B
Two equivalent non-bonding electron pairs at B:
HX
HX
One conformer
Two non-equivalent electron pairs at B :
HX
HX
HX
HX
Two conformers

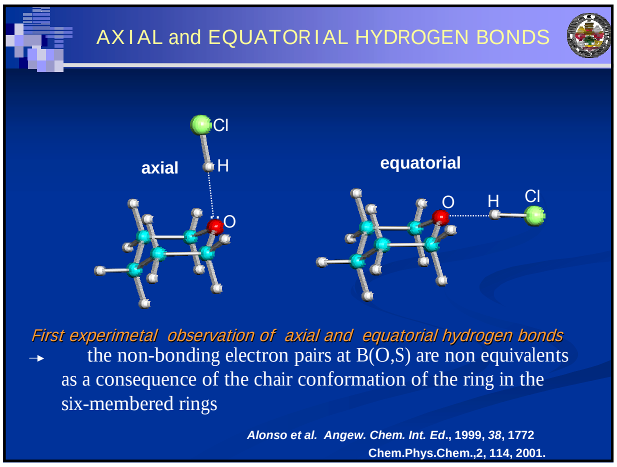
AXIAL and EQUATORIAL HYDROGEN BONDS
axial
equatorial
Cl
H
O
O
H
Cl
First experimental observation of axial and equatorial hydrogen bonds
→ the non-bonding electron pairs at B(O,S) are non equivalents as a consequence of the chair conformation of the ring in the six-membered rings
Alonso et al. Angew. Chem. Int. Ed., 1999, 38, 1772
Chem.Phys.Chem.,2, 114, 2001.

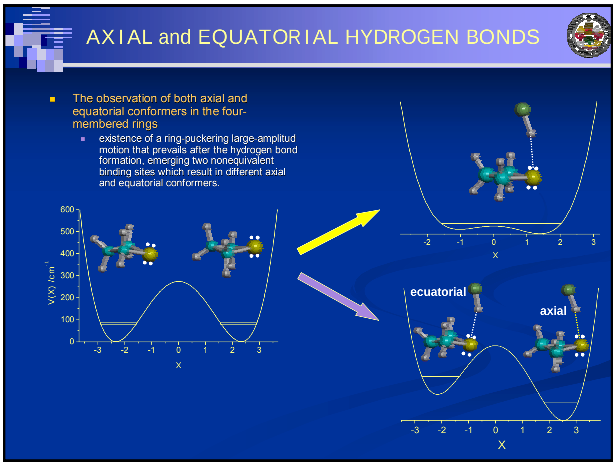
AXIAL and EQUATORIAL HYDROGEN BONDS
The observation of both axial and equatorial conformers in the four-membered rings
existence of a ring-puckering large-amplitud motion that prevails after the hydrogen bond formation, emerging two nonequivalent binding sites which result in different axial and equatorial conformers.
V(X) /cm-1
600
500
400
300
200
100
0
x
ecuatorial
axial
x

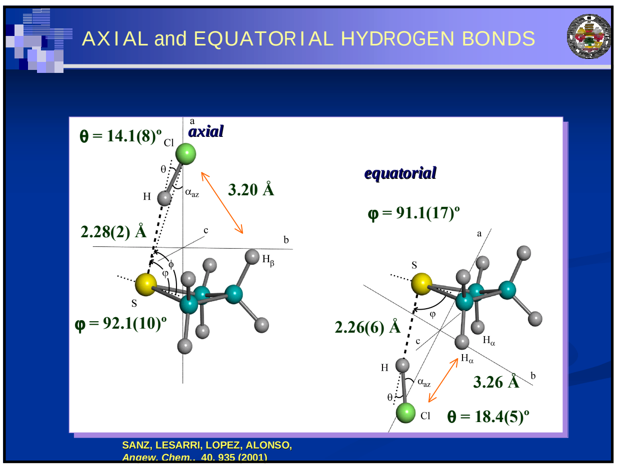
AXIAL and EQUATORIAL HYDROGEN BONDS
θ = 14.1(8)°
axial
3.20 Å
2.28(2) Å
φ = 92.1(10)°
equatorial
φ = 91.1(17)°
2.26(6) Å
3.26 Å
θ = 18.4(5)°
SANZ, LESARRI, LOPEZ, ALONSO,
Angew. Chem., 40, 935 (2001)

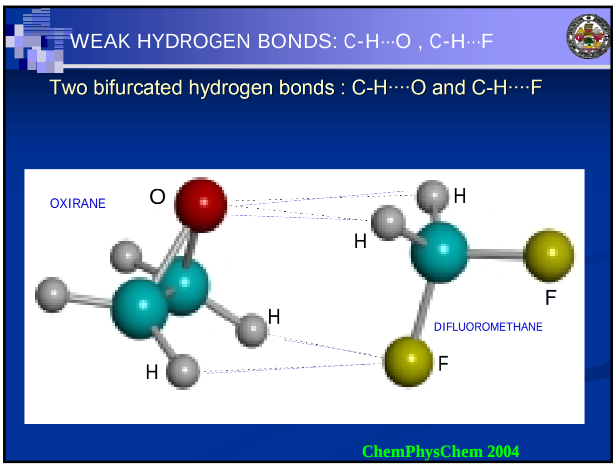
WEAK HYDROGEN BONDS: C-H···O , C-H···F
Two bifurcated hydrogen bonds : C-H····O and C-H····F
OXIRANE
O
H
H
H
H
F
F
DIFLUOROMETHANE
ChemPhysChem 2004

WEAK HYDROGEN BONDS: C-H···O , C-H···F

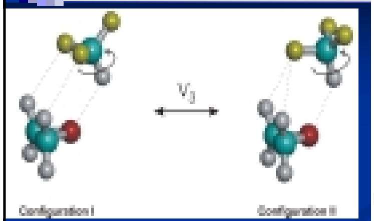

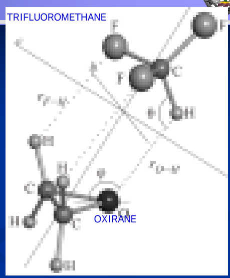

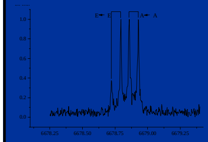

Three weak hydrogen bonds, one C-H···O and two C-H···F-H, establish the global minimum configuration of the oxirane···trifluoromethane adduct. The trifluoromethyl group can rotate almost freely (V3 = 0.55 kJ/mol) around its C3 symmetry axes.

Alonso et al.JACS, 2004

WEAK HYDROGEN BONDS: C-H···π

*Weak Hydrogen Bond Complex stabilized by a CH···π weak hydrogen bond. is a symmetric top.

* Both species are characterized by an almost free rotation of the two subunits with respect to each other. The estimated dissociation energy is 8.4 kJ/mol.

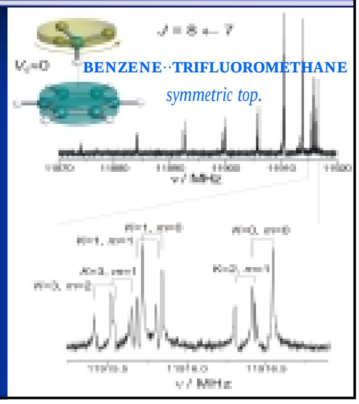

MICROSOLVATION: The formamide ···$(H_2O)_n$ *(n=1,2) clusters*

We have analyzed the rotational spectra of formamide-$(H_2O)_n$ clusters:

1) To characterize the different 1:1 and most stable 1:2 conformers.

2) To search for evidences of cooperative effects such as *polarization enhanced* or *resonance assisted* hydrogen bonding

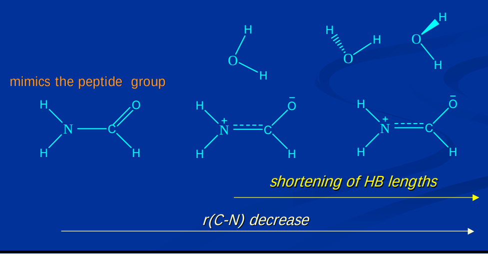

MICROSOLVATION: The formamide···$(H_2O)_n$ *(n=1,2) clusters*

1:1a The most stable conformer of the formamide-H_2O complex (), is stabilized by two hydrogen bonds O-H···O=C and N-H···O with water closing a cycle structure.

1:1b At the CO site the water acts as a proton donor bonded through the lone-pair of the oxygen atom in the carbonyl group.

1:1c At the NH site the water acts as an acceptor through the anti-hydrogen of the amino group.

1:2a Closed Cyclic structure with two water molecules establishing three hydrogen bonds.

interactions of water with the peptide functional group

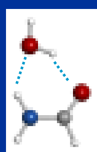

1:1a

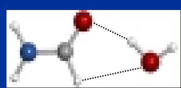

1:1b

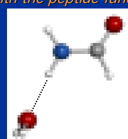

1:1c

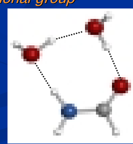

1:2a

Formamide ···H_2O 1:1a

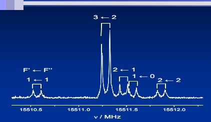

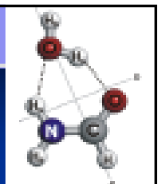

	Parent[a]	NH_2-^{13}COH ···(H_2O)	$^{15}NH_2$-COH ···(H_2O)	ND_sH_a-COH ···(H_2O)	NH_sD_a-COH ···(H_2O)	NH_2-COH ···$(H_2{}^{18}O)$	NH_2-COH ···(D_bH_cO)	NH_2-COH ···(H_bD_cO)
A/ MHz	11227.9330(23)	11224.4801(33)	10925.1667(27)	10844.4309(24)	10419.4158(49)	11221.9584(35)	11191.9592(21)	11140.3424(36)
B/ MHz	4586.9623(16)	4528.4531(13)	4565.9951(10)	4588.54771(69)	4514.1426(14)	4286.04140(99)	4287.0567(14)	4520.03865(10)
C/ MHz	3258.8277(12)	3228.9331(11)	3222.31874(95)	3226.77112(64)	3151.8641(13)	3103.50898(94)	3105.3851(14)	3218.02144(10)
Δ / u Å^2	-0.10814(41)	-0.10973(41)	-0.10439(39)	-0.12118(37)	-0.11529(44)	-0.10644(44)	-0.29761(44)	-0.12682(40)
Δ_J / kHz	7.844(70)	[7.844][c]	[7.844]	[7.844]	[7.844]	[7.844]	[7.844]	[7.844]
Δ_{JK}/ kHz	24.24(48)	[24.24]	[24.24]	[24.24]	[24.24]	[24.24]	[24.24]	[24.24]
Δ_K / kHz	[0.0]	[0.0]	[0.0]	[0.0]	[0.0]	[0.0]	[0.0]	[0.0]
δ_J / kHz	2.728(58)	[2.728]	[2.728]	[2.728]	[2.728]	[2.728]	[2.728]	[2.728]
δ_K / kHz	[0.0]	[0.0]	[0.0]	[0.0]	[0.0]	[0.0]	[0.0]	[0.0]
χ_{aa}/ MHz	1.3321(37)	1.3377(69)		1.3571(36)	1.3653(73)	1.3391(52)	1.3457(31)	1.3493(64)
χ_{bb}/ MHz	2.0371(20)	2.0334(64)		2.0381(20)	2.0485(41)	2.0271(28)	2.0333(17)	2.0413(26)
χ_{cc}/ MHz	-3.3693(96)	-3.371(26)		-3.3951(96)	-3.415(20)	-3.366(14)	-3.3791(81)	-3.391(14)
σ / kHz		4.9	2.6	3.9	8.2	5.7	6.6	6.0
N		15	5	21	21	21	21	21

Formamide ···H_2O 1:1b

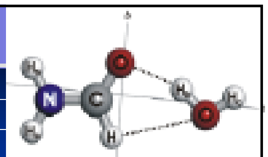

	0	1	MP2/6-311++G(d,p)
A / MHz[a]	26170.8(61)[d]		25970
B / MHz	2682.97653(65)	2682.97837(68)	2684
C / MHz	2433.84992(64)	2433.84900(63)	2438
Δ_J / kHz	7.6202(147)		
Δ_{JK} / kHz	-0.29706(38)		
Δ_K / kHz	[0.0][e]		
δ_J / kHz	1.3691 (133)		
δ_K / kHz	[0.0]		
χ_{aa} / MHz	1.8625(22)		
χ_{bb} / MHz	1.7393(39)		
χ_{cc} / MHz	-3.6018(39)		
σ / kHz	3.3		
N	66		

μ_a- and μ_b-type spectra
^{14}N quadrupole HFS
Tunneling Splittings (kHz)

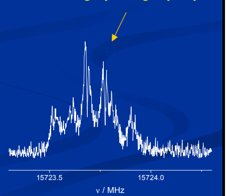

Formamide $\cdots H_2O$ 1:1c

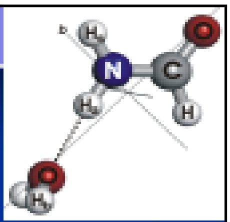

	a	b	MP2/6-311++G(d,p)
A / MHz [a]	[35288][b]		35288
B / MHz	2083.6104(127)[c]	2084.6949(126)	2073
C / MHz	1949.3157(126)	1949.7631(122)	1979
Δ / u Å^2			
χ_{aa} / MHz	1.5068(47)		
χ_{bb} / MHz	1.23(34)		
χ_{cc} / MHz	-2.73(34)		
σ / kHz	2.3		
N	26		

μ_a- and μ_b-type spectra
^{14}N quadrupole HFS
Tunneling Splittings (MHz)

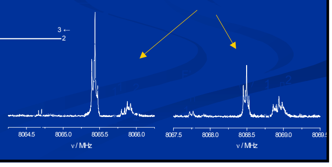

Formamide$\cdots(H_2O)_2$ 1:2 a

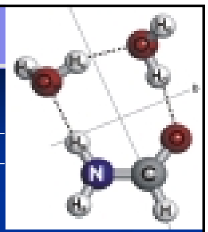

	Parent	NH_2-^{13}COH $\cdots(H_2O)_2$	$^{15}NH_2$-COH $\cdots(H_2O)_2$	ND_sH_a-COH $\cdots(H_2O)_2$
A/ MHz [a]	4384.3559(50)[b]	4384.34925(250)	4334.6691(20)	4321.9095(33)
B/ MHz	2630.4957(158)	2590.06990(52)	2611.20693(44)	2630.42759(305)
C/ MHz	1651.1140(125)	1635.09880(34)	1636.47057(26)	1642.26244(72)
Δ_J / kHz	2.08(68)	[2.08]	[2.08]	[2.08]
Δ_{JK}/ kHz	16.3(3.8)	[16.3]	[16.3]	[16.3]
Δ_K / kHz	[0.0][c]	[0.0]	[0.0]	[0.0]
δ_J / kHz	0.565(152)	[0.565]	[0.565]	[0.565]
δ_K / kHz	18.1(5.7)	[18.1]	[18.1]	[18.1]
χ_{aa}/ MHz	1.0739(34)	1.0608(69)		1.0467(168)
χ_{bb}/ MHz	2.0063(45)	2.0220(101)		2.0141(208)
χ_{cc}/ MHz	-3.0802(45)	-3.0828(101)		-3.0607(208)
σ / kHz	3.9	4.0	2.0	5.1
N	37	20	8	13

Formamide$\cdots(H_2O)_2$ 1:2 a

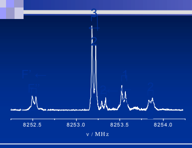

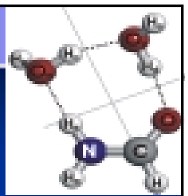

	NH_2-COH $\cdots(H_2{}^{18}O_w)(H_2O)$	NH_2-COH $\cdots(D_bH_cO)(H_2O)$	NH_2-COH $\cdots(H_bD_cO)(H_2O)$	NH_2-COH $\cdots(H_2O)(H_2{}^{18}O_v)$	NH_2-COH $\cdots(H_2O)(D_dH_eO)$	NH_2-COH $\cdots(H_2O)(H_dD_eO)$
A/ MHz[a]	4257.87728(396) [b]	4267.05691(370)	4380.5341(46)	4258.42155(312)	4313.55882(347)	4230.04111(313)
B/ MHz	2550.81170(119)	2554.07174(293)	2582.15945(359)	2558.17803(94)	2625.27494(238)	2575.60939(225)
C/ MHz	1601.76873(42)	1609.03594(50)	1631.64517(66)	1604.74185(33)	1639.01599(51)	1611.42773(41)
Δ_J / kHz	[2.08][c]	[2.08]	[2.08]	[2.08]	[2.08]	[2.08]
Δ_{JK}/ kHz	[16.3]	[16.3]	[16.3]	[16.3]	[16.3]	[16.3]
Δ_K / kHz	[0.0]	[0.0]	[0.0]	[0.0]	[0.0]	[0.0]
δ_J / kHz	[0.565]	[0.565]	[0.565]	[0.565]	[0.565]	[0.565]
δ_K / kHz	[18.1]	[18.1]	[18.1]	[18.1]	[18.1]	[18.1]
χ_a/ MHz	1.0493(91)	0.9975(193)	1.0447(234)	1.0754(75)	1.0717(181)	1.0575(123)
χ_b/ MHz	2.0142(147)	2.0295(238)	2.0334(290)	2.0009(121)	2.0286(225)	2.0108(177)
χ_c/ MHz	-3.0634(147)	-3.0269(238)	-3.0782(290)	-3.0763(121)	-3.1002(225)	-3.0684(177)
σ / kHz	6.4	5.9	7.2	5.2	5.5	5.0
N	21	17	16	21	16	18

Structures : Formamide

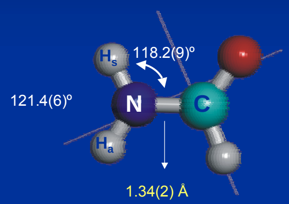

	r_s
$r_{(C-N)}$/ Å	1.343(21)
$r_{(C-Hs)}$/ Å	1.0020(84)
$r_{(C-Ha)}$/ Å	0.9907(72)
∠(C-N-H_s)/ º	118.23(86)
∠(C-N-H_a)/ º	120.4(1.2)
∠(H_a-N-H_s)/ º	121.37(64)

Structures : Formamide 1:1a

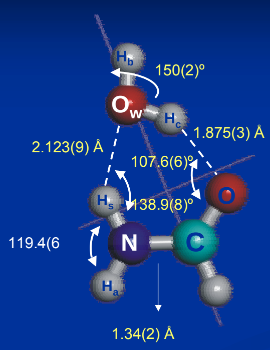

	r_s
$r_{(C-N)}$/ Å	1.341(15)
$r_{(C-Hs)}$/ Å	0.9321(93)
$r_{(C-Ha)}$/ Å	0.9753(79)
$r_{(Ow-Hb)}$/ Å	0.919(25)
$r_{(Ow-Hc)}$/ Å	1.022(11)
$r_{(Ow\cdots Hs)}$/ Å	2.1234(91)
$r_{(O\cdots Hc)}$/ Å	1.8745(33)
∠(C-N-H_s)/ º	119.56(58)
∠(C-N-H_a)/ º	120.6(1.2)
∠(H_a-N-H_s)/ º	119.37(64)
∠(H_b-O_w-H_c)/ º	106.1(2.9)
∠(N-$H_s\cdots O_w$)/ º	138.87(75)
∠(C-O$\cdots H_c$)/ º	107.56(56)
∠($H_s\cdots O_w$-H_c)/ º	77.34(56)
∠(H_b-O_w-$H_c\cdots H_s$)/ º	150.4(2.4)

Structures : Formamide 1:2a

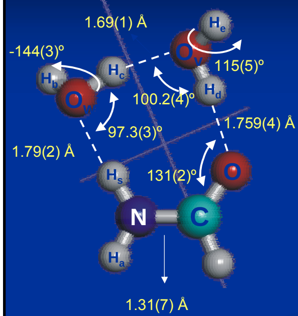

	r_s
$r_{(C-N)}$/ Å	1.307(72)
$r_{(C-Hs)}$/ Å	1.126(21)
$r_{(Ow-Hb)}$/ Å	0.970(30)
$r_{(Ow-Hc)}$/ Å	1.109(10)
$r_{(Ov-He)}$/ Å	0.961(26)
$r_{(Ov-Hd)}$/ Å	1.0243(51)
$r_{(Ow\cdots Hs)}$/ Å	1.792(20)
$r_{(Ov\cdots Hc)}$/ Å	1.6852(98)
$r_{(O\cdots Hd)}$/ Å	1.7590(40)
∠(C-N-H_s)/ º	121.2(1.9)
∠(H_b-O_w-H_c)/ º	108.7(2.2)
∠(H_e-O_v-H_d)/ º	106.8(2.4)
∠(N-$H_s\cdots O_w$)/ º	171.2(4.1)
∠($H_s\cdots O_w$-H_c)/ º	97.26(25)
∠(O_w-$H_c\cdots O_v$)/ º	157.5(2.2)
∠($H_c\cdots O_v$-H_d)/ º	100.15(42)
∠(C-O$\cdots H_d$)/ º	130.7(2.1)
∠(H_b-O_w-$H_c\cdots H_s$)/ º	-144.4(3.2)
∠(H_e-O_v-$H_d\cdots H_s$)/ º	114.7(4.5)

Cooperative Effects

* No evidences *resonance assisted* hydrogen bonding

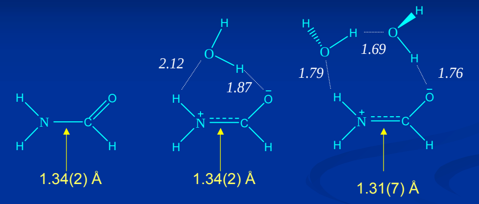

r(C-N) decrease

* Evidences of *polarization enhanced* hydrogen bonding

→ *shortening of HB lengths*

NEUROTRANSMITTERS

Ethylamine side chain

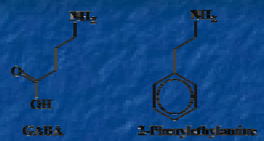

Molecules which mediate the connections between nerve cells belong to the family of neurotransmitter. Many share a common structural motif

Ethanolamine side chain

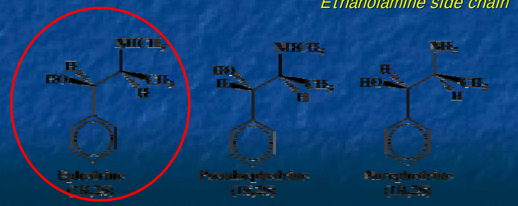

EPHEDRINE

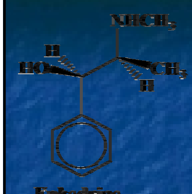

Is representative of a wide family of neurotransmitters comprising an ethanolamine side chain attached to an aromatic ring.

→ Molecular Conformation plays a crucial role for the understanding of the biological function

The torsional flexibility of the side chain results in an unusual great number of low energy conformers whose relative stability is controlled by intramolecular interactions involving hydrogen bonding.

→

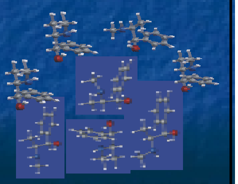

Ephedrine: Lower-energy Conformers

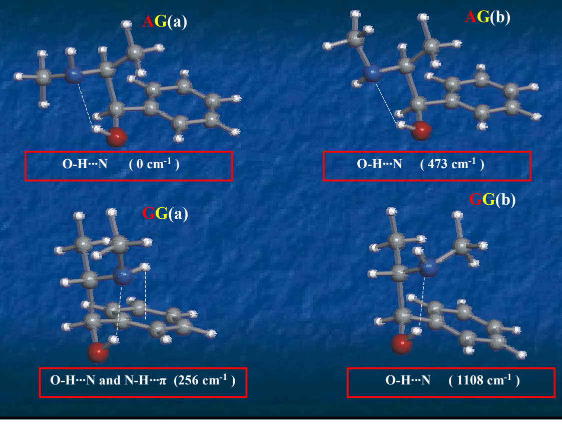

MB-FTMW

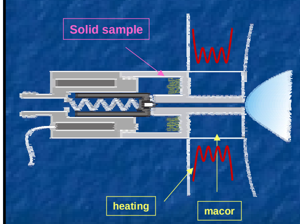

GEM. Valladolid

EPHEDRINE

Spectroscopic Parameters	AG(a)		GG(a)		AG(b)	
	AB-INITIO	EXPERIMENTAL	AB-INITIO	EXPERIMENTAL	AB-INITIO	EXPERIMENTAL
A / MHz	2014.4	1998.63822 (35)	1565.7	1568.24526 (49)	2112.1	2115.87705 (59)
B / MHz	532.8	529.549500 (41)	597.1	592.448419 (73)	507.2	503.794257 (40)
C / MHz	504.6	500.160014 (41)	579.3	572.416089 (62)	480.0	475.173363 (51)
χ_{aa} / MHz	2.63	2.5347 (13)	2.51	2.447 (12)	2.70	2.564 (17)
χ_{bb} / MHz	-3.26	-2.7436 (17)	-2.90	-3.2045 (75)	-4.83	-4.622 (11)
χ_{cc} / MHz	0.63	0.2089 (17)	0.39	0.7575 (75)	2.14	2.058 (11)

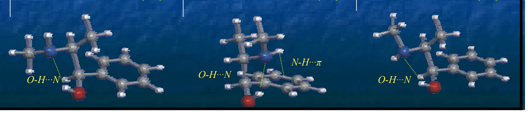

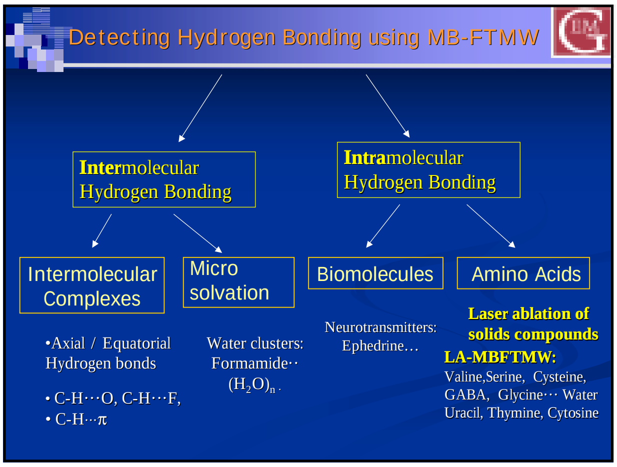
Detecting Hydrogen Bonding using MB-FTMW
Intermolecular Hydrogen Bonding
Intramolecular Hydrogen Bonding
Intermolecular Complexes
Micro solvation
Biomolecules
Amino Acids
•Axial / Equatorial Hydrogen bonds
• C-H···O, C-H···F,
• C-H···π
Water clusters: Formamide·· $(H_2O)_n$
Neurotransmitters: Ephedrine…
Laser ablation of solids compounds
LA-MBFTMW:
Valine,Serine, Cysteine, GABA, Glycine··· Water Uracil, Thymine, Cytosine

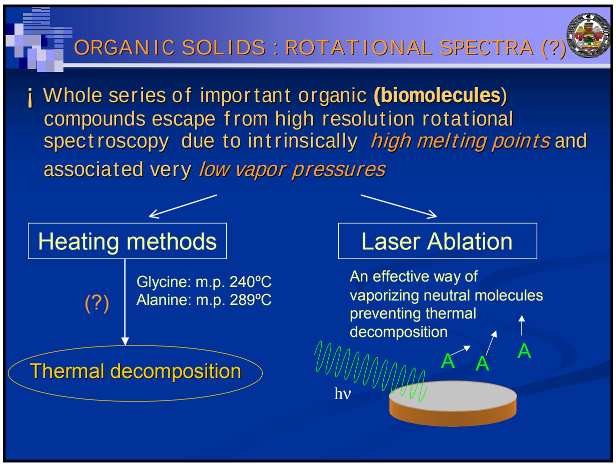
ORGANIC SOLIDS : ROTATIONAL SPECTRA (?)
¡ Whole series of important organic **(biomolecules)** compounds escape from high resolution rotational spectroscopy due to intrinsically *high melting points* and associated very *low vapor pressures*
Heating methods
Laser Ablation
Glycine: m.p. 240ºC
Alanine: m.p. 289ºC
(?)
Thermal decomposition
An effective way of vaporizing neutral molecules preventing thermal decomposition
A
A
A
hν

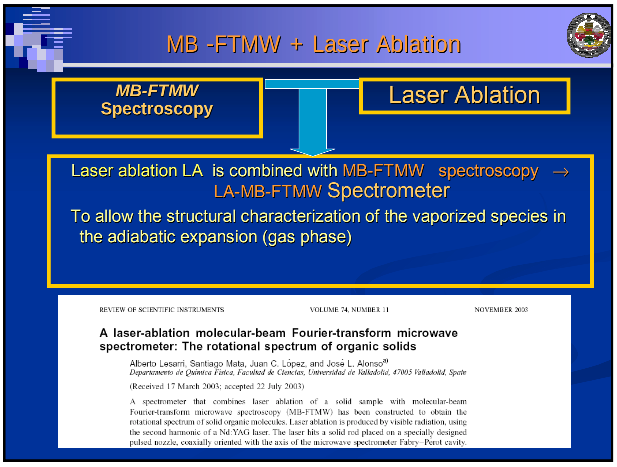
MB -FTMW + Laser Ablation
MB-FTMW Spectroscopy
Laser Ablation
Laser ablation LA is combined with MB-FTMW spectroscopy → LA-MB-FTMW Spectrometer
To allow the structural characterization of the vaporized species in the adiabatic expansion (gas phase)
REVIEW OF SCIENTIFIC INSTRUMENTS VOLUME 74, NUMBER 11 NOVEMBER 2003
A laser-ablation molecular-beam Fourier-transform microwave spectrometer: The rotational spectrum of organic solids
Alberto Lesarri, Santiago Mata, Juan C. López, and José L. Alonso
Departamento de Química Física, Facultad de Ciencias, Universidad de Valladolid, 47005 Valladolid, Spain
(Received 17 March 2003; accepted 22 July 2003)
A spectrometer that combines laser ablation of a solid sample with molecular-beam Fourier-transform microwave spectroscopy (MB-FTMW) has been constructed to obtain the rotational spectrum of solid organic molecules. Laser ablation is produced by visible radiation, using the second harmonic of a Nd:YAG laser. The laser hits a solid rod placed on a specially designed pulsed nozzle, coaxially oriented with the axis of the microwave spectrometer Fabry–Perot cavity.

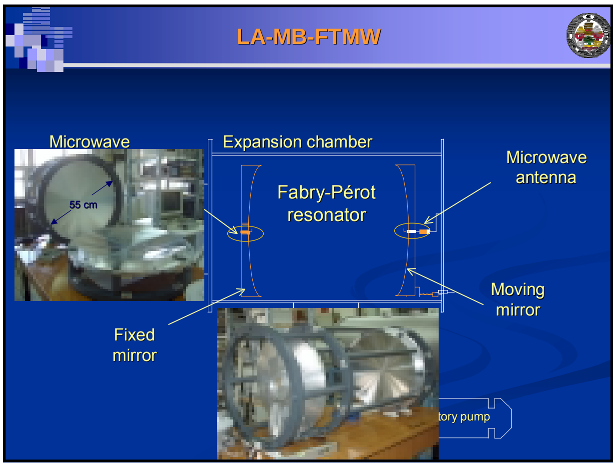
LA-MB-FTMW
Microwave
Expansion chamber
55 cm
Fabry-Pérot resonator
Microwave antenna
Moving mirror
Fixed mirror
tory pump

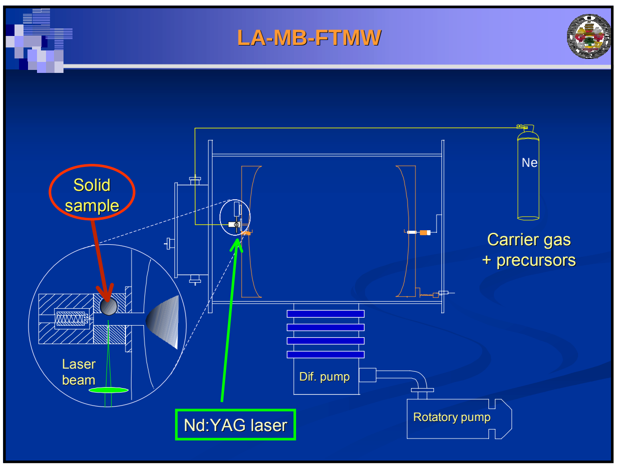
LA-MB-FTMW
Solid sample
Ne
Carrier gas + precursors
Laser beam
Dif. pump
Nd:YAG laser
Rotatory pump


LA-MB-FTMW: Ablation nozzle
Valladolid 2005
Sample compartment
nozzle
solid

LA-MB-FTMW

LA-MB-FTMW : Experimental Sequence

1. Each cycle starts with a gas pulse of Ne or Ar as carrier gas ⇒

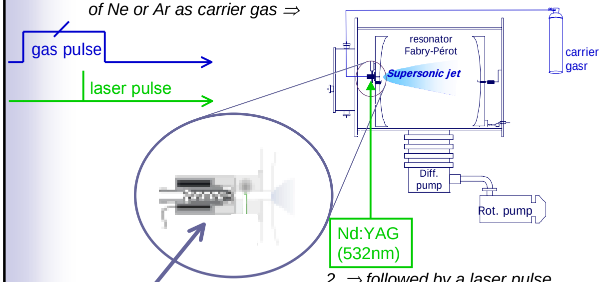

2. ⇒ followed by a laser pulse generating the ablations products which are seeded in carrier gas
→ Supersonic expansion (jet).

LA-MB-FTMW : Experimental Sequence

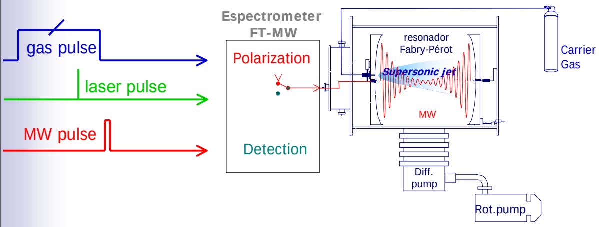

3. A very short microwave induces a macroscopic
Polarization

LA-MB-FTMW : Experimental Sequence

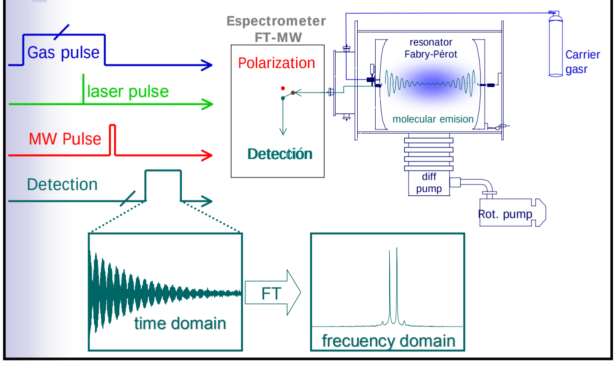

Why Amino Acids in the Gas-Phase ?

- The great torsional flexibility of amino acids results in an unusual great number of stable conformers of low energy whose relative stability is contolled by intramolecular interactions.

⇨The intrinsic conformational preferences are only revealed in isolation conditions in the gas phase.

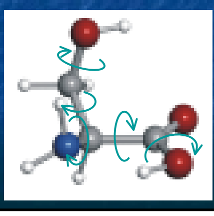

serine up to 324 predicted conformers

Why Amino Acids in the Gas-Phase ?

- Amino Acids in their natural condensed phases are stabilized as by strong intermolecular interactions as zwitterions (i.e., a bipolar ionized form ($^{+}H_3N$-CH(R)-COO^{-}) which does not occur in the polypeptide chain →The structural research of the neutral aminoacids should be conducted in gas phase where the they present an unsolvated neutral form HN-CH(R)-COOH which represents the best approximation of an amino acid residue in a polipedtide chain.

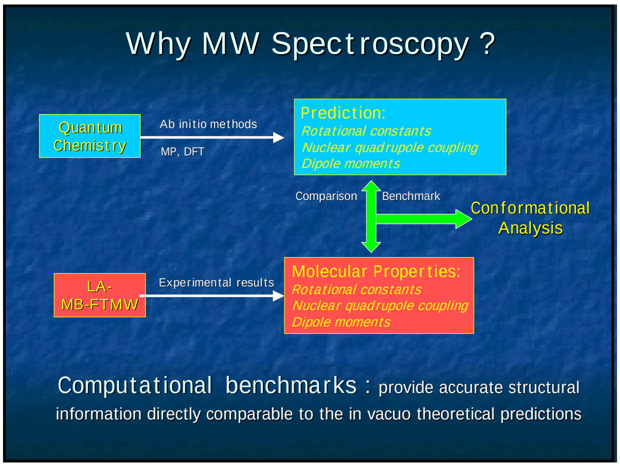
Why MW Spectroscopy ?
Quantum Chemistry
Ab initio methods
MP, DFT
Prediction:
Rotational constants
Nuclear quadrupole coupling
Dipole moments
Comparison
Benchmark
Conformational Analysis
LA-MB-FTMW
Experimental results
Molecular Properties:
Rotational constants
Nuclear quadrupole coupling
Dipole moments
Computational benchmarks : provide accurate structural information directly comparable to the in vacuo theoretical predictions

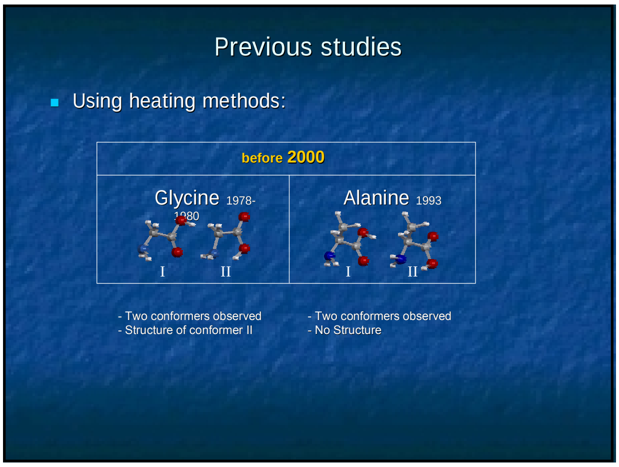
Previous studies
Using heating methods:
before 2000
Glycine 1978-1980
Alanine 1993
I
II
I
II
- Two conformers observed
- Structure of conformer II
- Two conformers observed
- No Structure

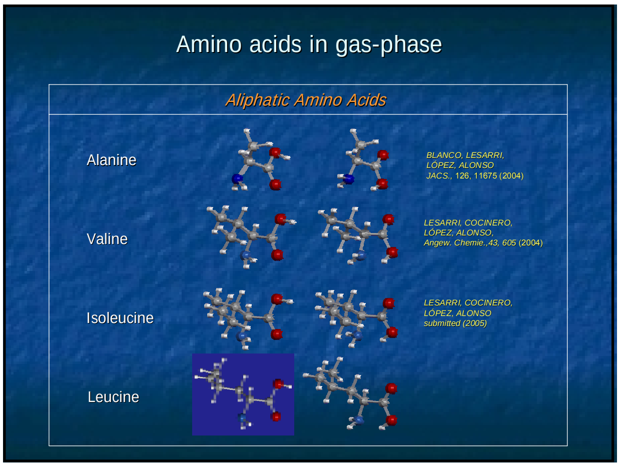
Amino acids in gas-phase
Aliphatic Amino Acids
Alanine
BLANCO, LESARRI, LÓPEZ, ALONSO
JACS., 126, 11675 (2004)
Valine
LESARRI, COCINERO, LÓPEZ, ALONSO,
Angew. Chemie.,43, 605 (2004)
Isoleucine
LESARRI, COCINERO, LÓPEZ, ALONSO
submitted (2005)
Leucine

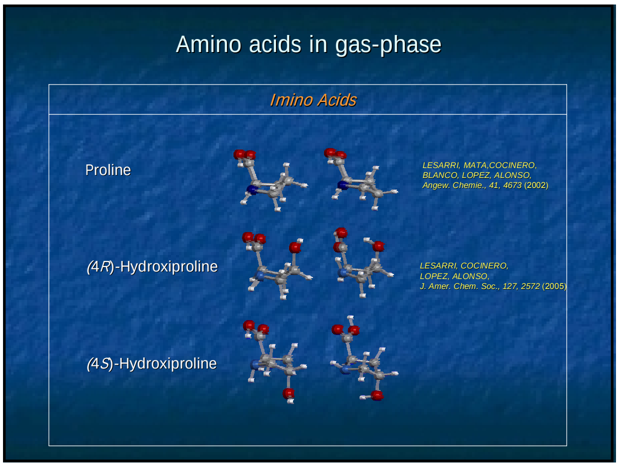
Amino acids in gas-phase
Imino Acids
Proline
LESARRI, MATA,COCINERO, BLANCO, LOPEZ, ALONSO,
Angew. Chemie., 41, 4673 (2002)
(4R)-Hydroxiproline
LESARRI, COCINERO, LOPEZ, ALONSO,
J. Amer. Chem. Soc., 127, 2572 (2005)
(4S)-Hydroxiproline

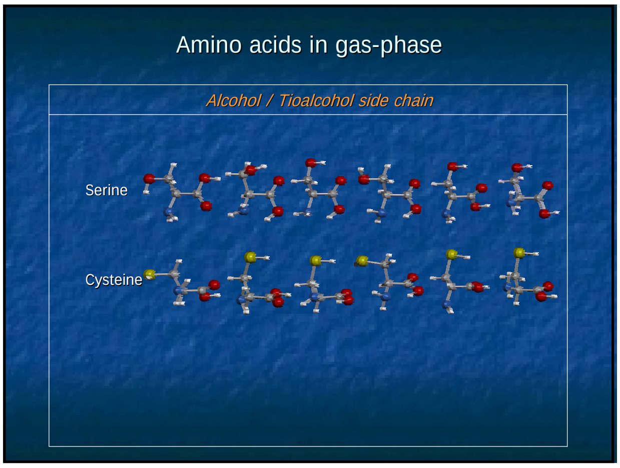
Amino acids in gas-phase
Alcohol / Tioalcohol side chain
Serine
Cysteine

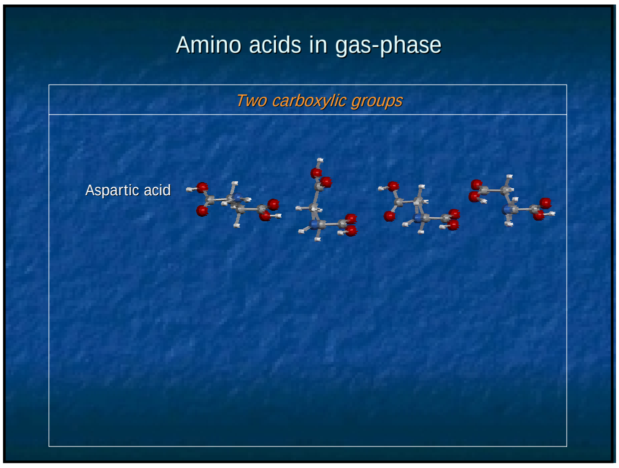
Amino acids in gas-phase
Two carboxylic groups
Aspartic acid

Non-coded Amino acids in gas-phase

α-Amino acids

N,N-dimetil glycine

Sarcosine

α-Aminobutyric

Phenylglycine

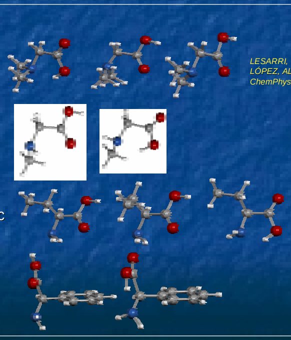

LESARRI, COCINERO, LÓPEZ, ALONSO, ChemPhysChem. In press (2005)

Non-coded Amino acids in gas-phase

β- and γ-Amino acids

β-Alanine

β-Aminobutyric

γ-Aminobutyric GABA

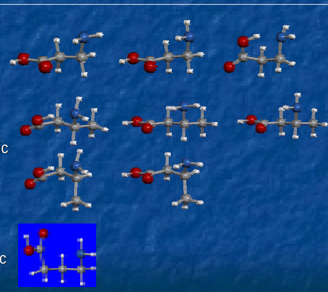

Amino Acids in space ?

Laboratory → Radiotelescope

Spectroscopic parameters

- Presence in the interestellar medium: ¿Origin of life?

8 átomos	9 átomos	10 átomos	11 átomos	12 átomos	13 átomos
CH_3C_3N	CH_3C_4H	CH_3C_5N ?	HC_9N	C_6H_6 ?	$HC_{11}N$
$HCOOCH_3$	CH_3CH_2CN	$(CH_3)_2CO$			
CH_3COOH	$(CH_3)_2O$	$(CH_2OH)_2$?			
C_7H	CH_3CH_2OH	$H_2NCH_2CO_2H$ **Glicina ?**			
H_2C_6	HC_7N	CH_3CH_2CHO			
CH_2OHCHO	C_8H				
$l\text{-}HC_6H$?					
CH_2CHCHO ?					

136 molecules
(December 2004)

Glycine ?,
Ác. Fórmico, ac. acético, acrilonitrilo, Etilenglicol, benceno?

SERINE

The introduction of the ethoxy group adds two rotors and the additional donor-acceptor hydrogen bonding capabilities of the hydroxy group

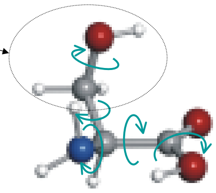

The exploration of the conformational landscape of serine by ab initio quantum chemical calculations ⇒ *up to 324 predicted conformations*

Gronert et al JACS 117 (1995)

α - Amino Acids

- The conformational behavior is conditioned by the potential formation of 3 different types of intramolecular hydrogen bonds:
  - Type I: amine-to-carbonyl oxygen (NH···O=C)

Conf. I

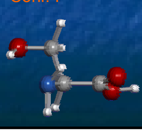

α - Amino Acids

- The conformational behavior is conditioned by the potential formation of 3 different types of intramolecular hydrogen bonds:
  - Type I: amine-to-carbonyl oxygen (NH···O=C)
  - Type II: N lone pair – Hydroxyl hydrogen (N···H-O)

Conf. I Conf. II

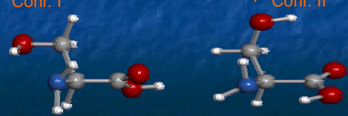

α - Amino Acids

- The conformational behavior is conditioned by the potential formation of 3 different types of intramolecular hydrogen bonds:
  - Type I: amine-to-carbonyl oxygen (NH···O=C)
  - Type II: N lone pair – Hydroxyl hydrogen (N···H-O)
  - Type III: H amine group – Hydroxyl oxygen (NH···O-H)

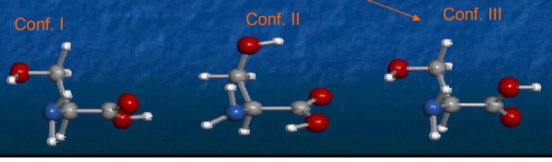

Amino Acids : Side chain orientation

- The etoxy group can additionally establish three orientations of the hydroxy group (a, b, c) for each conformer. The energy ordering of these configurations could depend on the backbone conformation.

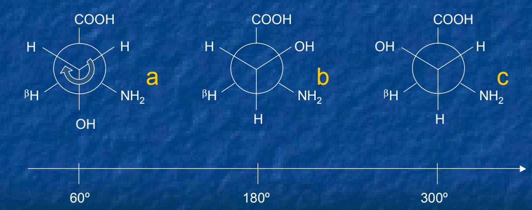

SERINE : Lower Energy Conformers

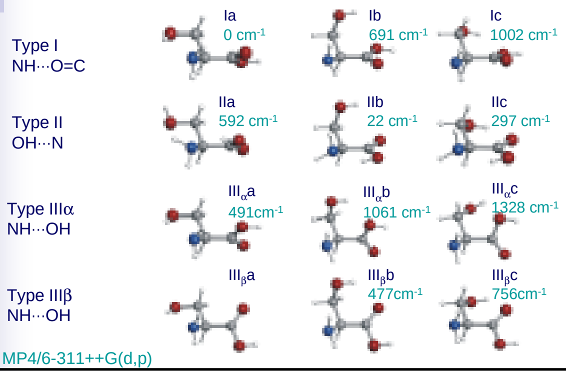

MP4/6-311++G(d,p)

SERINE : Rotational Spectrum

* a-type R-Branch transitions of an asymmetric rotor were assigned.

* All the transitions are splitted in several components attributable to the nuclear hyperfine interactions of a single ^{14}N nucleus (I=1).

A / MHz	4479.0320 (12)
B / MHz	1830.16170 (25)
C / MHz	1443.79545 (28)
Δ_J / kHz	0.2006 (61)
Δ_{JK} / kHz	1.73 (17)
Δ_K / kHz	[0.0]
δ_J / kHz	[0.0]
δ_K / kHz	[0.0]
χ_{aa} / MHz	-4.3023 (27)
χ_{bb} / MHz	2.82359 (63)
χ_{cc}/ MHz	1.4788 (46)
σ / kHz	3.0
N	53

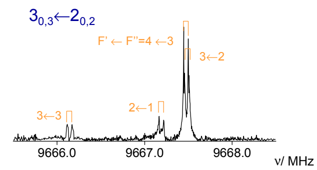

$$H = H^A_R + H_Q$$

Watson Semirigid Rotor

Nuclear Quadrupole Coupling Term

SERINE

	Ia		IIb		IIc		IIa		$III_\beta b$		$III_\beta c$	
	MP2	Exp.	MP2	Exp.	MP2	Exp.	MP2	Exp.	MP2	Exp.	MP2	Exp.
A / MHz	4481	4479.03	3544		3656		4522		3934		3519	
B / MHz	1824	1830.16	2395		2378		1850		2249		2331	
C / MHz	1452	1443.79	1748		1518		1479		1667		1580	
χ_{aa} / MHz	-4.66	-4.302	-3.67		-3.89		-0.44		-0.65		-1.08	
χ_{bb} / MHz	2.92	2.823	2.21		2.13		2.05		-0.53		-0.75	
χ_{cc}/ MHz	1.74	1.478	1.44		1.75		-1.61		1.19		1.82	
ΔE / cm-1	0		22		297		529		477		756	

Ia

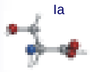

SERINE : Rotational Spectrum

* Another series of a-type R-Branch transitions of an asymmetric rotor were assigned.

* All the transitions are splitted in several components attributable to the nuclear hyperfine interactions of a single ^{14}N nucleus (I=1).

A / MHz	3557.20088 (25)
B / MHz	2380.37208 (40)
C / MHz	1740.92458 (10)
Δ_J / kHz	0.8646 (98)
Δ_{JK} / kHz	[0.0]
Δ_K / kHz	[0.0]
δ_J / kHz	[0.0]
δ_K / kHz	[0.0]
χ_{aa} / MHz	-3.4616 (19)
χ_{bb} / MHz	2.07970 (93)
χ_{cc}/ MHz	1.3819 (47)
σ / kHz	3.3
N	74

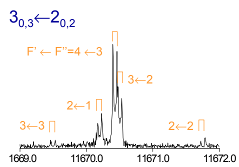

SERINE

	Ia		IIb		IIc		IIa		III$_\beta$b		III$_\beta$c	
	MP2	Exp.	MP2	Exp.	MP2	Exp.	MP2	Exp.	MP2	Exp.	MP2	Exp.
A / MHz	4481	4479.03	3544	3557.20	3656		4522		3934		3519	
B / MHz	1824	1830.16	2395	2380.37	2378		1850		2249		2331	
C / MHz	1452	1443.79	1748	1740.92	1518		1479		1667		1580	
χ_{aa} / MHz	-4.66	-4.302	-3.67	-3.461	-3.89		-0.44		-0.65		-1.08	
χ_{bb} / MHz	2.92	2.823	2.21	2.079	2.13		2.05		-0.53		-0.75	
χ_{cc}/ MHz	1.74	1.478	1.44	1.381	1.75		-1.61		1.19		1.82	
ΔE / cm^{-1}	0		22		297		529		477		756	

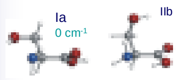

SERINE : Rotational Spectrum

* Another two series of a-type R-Branch transitions of an asymmetric rotor were assigned.

* All the transitions are splitted in several components attributable to the nuclear hyperfine interactions of a single ^{14}N nucleus (I=1).

A / MHz	3638.05784 (38)	4517.473 (17)
B / MHz	2387.89651 (99)	1846.99360 (30)
C / MHz	1519.18716 (36)	1463.79646 (31)
Δ_J / kHz	0.246 (34)	0.242 (10)
Δ_{JK} / kHz	[0.0]	[0.0]
Δ_K / kHz	[0.0]	[0.0]
δ_J / kHz	[0.0]	[0.0]
δ_K / kHz	[0.0]	[0.0]
χ_{aa} / MHz	-3.6527 (57)	-0.6066 (55)
χ_{bb} / MHz	2.06213 (26)	2.0723 (82)
χ_{cc}/ MHz	1.5906 (50)	-1.466 (30)
σ / kHz	2.5	2.2
N	24	24

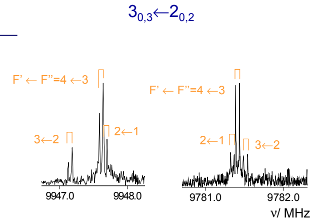

SERINE

	Ia		IIb		IIc		IIa		III$_\beta$b		III$_\beta$c	
	MP2	Exp.	MP2	Exp.	MP2	Exp.	MP2	Exp.	MP2	Exp.	MP2	Exp.
A / MHz	4481	4479.03	3544	3557.20	3656	3638.05	4522		3934		3519	
B / MHz	1824	1830.16	2395	2380.37	2378	2387.89	1850		2249		2331	
C / MHz	1452	1443.79	1748	1740.92	1518	1519.18	1479		1667		1580	
χ_{aa} / MHz	-4.66	-4.302	-3.67	-3.461	-3.89	-3.652	-0.44		-0.65		-1.08	
χ_{bb} / MHz	2.92	2.823	2.21	2.079	2.13	2.062	2.05		-0.53		-0.75	
χ_{cc}/ MHz	1.74	1.478	1.44	1.381	1.75	1.590	-1.61		1.19		1.82	
ΔE / cm^{-1}	0		22		297		529		477		756	

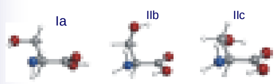

SERINE

	Ia		IIb		IIc		IIa		III$_\beta$b		III$_\beta$c	
	MP2	Exp.	MP2	Exp.	MP2	Exp.	MP2	Exp.	MP2	Exp.	MP2	Exp.
A / MHz	4481	4479.03	3544	3557.20	3656	3638.05	4522	4517.47	3934		3519	
B / MHz	1824	1830.16	2395	2380.37	2378	2387.89	1850	1846.99	2249		2331	
C / MHz	1452	1443.79	1748	1740.92	1518	1519.18	1479	1463.79	1667		1580	
χ_{aa} / MHz	-4.66	-4.302	-3.67	-3.461	-3.89	-3.652	-0.44	-0.606	-0.65		-1.08	
χ_{bb} / MHz	2.92	2.823	2.21	2.079	2.13	2.062	2.05	2.072	-0.53		-0.75	
χ_{cc}/ MHz	1.74	1.478	1.44	1.381	1.75	1.590	-1.61	-1.466	1.19		1.82	
ΔE / cm^{-1}	0		22		297		529		477		756	

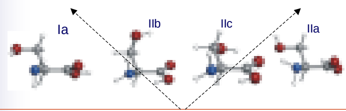

^{14}N nuclear quadrupolo coupling constants,which depend on the electronic environment around the amino nitrogen are extremely sensitive to the amino group orientation ⟶ UNIQUE IDENTIFIER

SERINE : Rotational Spectrum

* Another series of a-type R-Branch transitions of an asymmetric rotor were assigned.

* All the transitions are splitted in several components attributable to the nuclear hyperfine interactions of a single ^{14}N nucleus (I=1).

A / MHz	3931.7548 (76)
B / MHz	2242.76701 (70)
C / MHz	1664.53012 (11)
Δ_J / kHz	0.613 (11)
Δ_{JK} / kHz	[0.0]
Δ_K / kHz	[0.0]
δ_J / kHz	0.245 (11)
δ_K / kHz	[0.0]
χ_{aa} / MHz	-0.673 (14)
χ_{bb} / MHz	-0.456 (33)
χ_{cc}/ MHz	1.129 (84)
σ / kHz	2.4
N	23

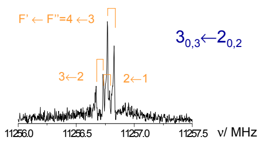

SERINE

	Ia		IIb		IIc		IIa		III$_\beta$b		III$_\beta$c	
	MP2	Exp.	MP2	Exp.	MP2	Exp.	MP2	Exp.	MP2	Exp.	MP2	Exp.
A / MHz	4481	4479.03	3544	3557.20	3656	3638.05	4522	4517.47	3934	3931.75	3519	
B / MHz	1824	1830.16	2395	2380.37	2378	2387.89	1850	1846.99	2249	2242.76	2331	
C / MHz	1452	1443.79	1748	1740.92	1518	1519.18	1479	1463.79	1667	1664.53	1580	
χ_{aa} / MHz	-4.66	-4.302	-3.67	-3.461	-3.89	-3.652	-0.44	-0.606	-0.65	-0.673	-1.08	
χ_{bb} / MHz	2.92	2.823	2.21	2.079	2.13	2.062	2.05	2.072	-0.53	-0.456	-0.75	
χ_{cc}/ MHz	1.74	1.478	1.44	1.381	1.75	1.590	-1.61	-1.466	1.19	1.129	1.82	
ΔE / cm^{-1}	0		22		297		529		477		756	

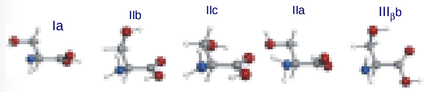

SERINE : Rotational Spectrum

* Another series of a-type R-Branch transitions of an asymmetric rotor were assigned.

* All the transitions are splitted in several components attributable to the nuclear hyperfine interactions of a single ^{14}N nucleus (I=1).

	principal
A / MHz	3510.4015 (35)
B / MHz	2321.90829 (24)
C / MHz	1584.38608 (32)
Δ_J / kHz	0.504 (11)
Δ_{JK} / kHz	[0.0]
Δ_K / kHz	[0.0]
δ_J / kHz	[0.0]
δ_K / kHz	[0.0]
χ_{aa} / MHz	-1.0486 (55)
χ_{bb} / MHz	-0.5637 (53)
χ_{cc} / MHz	1.612 (21)
σ / kHz	1.9
N	16

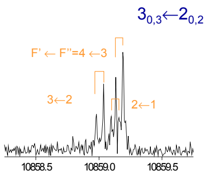

SERINE

	Ia		IIb		IIc		IIa		$III_\beta b$		$III_\beta c$	
	MP2	Exp.	MP2	Exp.	MP2	Exp.	MP2	Exp.	MP2	Exp.	MP2	Exp.
A / MHz	4481	4479.03	3544	3557.20	3656	3638.05	4522	4517.47	3934	3931.75	3519	3510.40
B / MHz	1824	1830.16	2395	2380.37	2378	2387.89	1850	1846.99	2249	2242.76	2331	2321.90
C / MHz	1452	1443.79	1748	1740.92	1518	1519.18	1479	1463.79	1667	1664.53	1580	1584.38
χ_{aa} / MHz	-4.66	-4.302	-3.67	-3.461	-3.89	-3.652	-0.44	-0.606	-0.65	-0.673	-1.08	-1.048
χ_{bb} / MHz	2.92	2.823	2.21	2.079	2.13	2.062	2.05	2.072	-0.53	-0.456	-0.75	-0.563
χ_{cc} / MHz	1.74	1.478	1.44	1.381	1.75	1.590	-1.61	-1.466	1.19	1.129	1.82	1.612
ΔE / cm^{-1}	0		22		297		529		477		756	

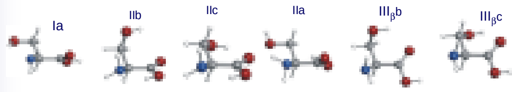

SERINE : Observed Conformers

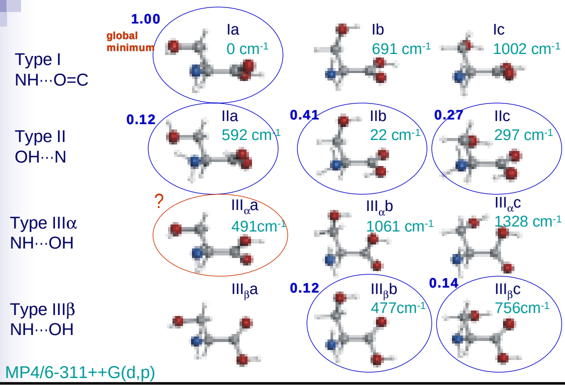

MP4/6-311++G(d,p)

Supersonic jets: "Missing" conformers

High interconformer barriers

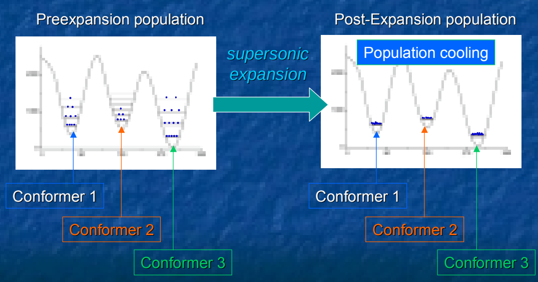

Supersonic jets: "Missing" conformers

Low interconformer barriers

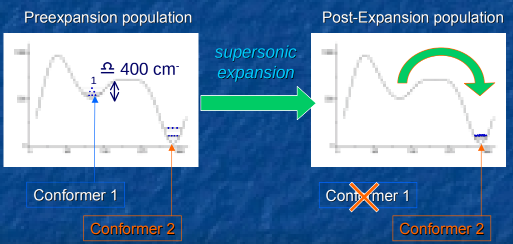

Conformer relaxation

Serine: Interconversion barriers

High interconformer barriers

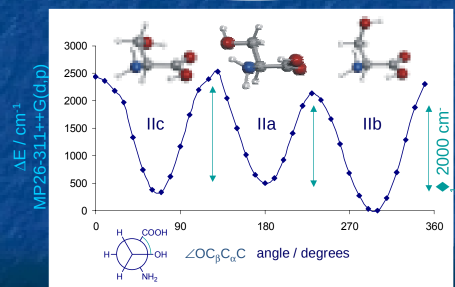

Serine: Interconversion barriers

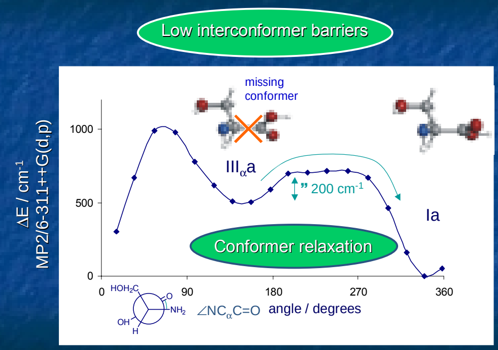

Cysteine : Observed Conformers

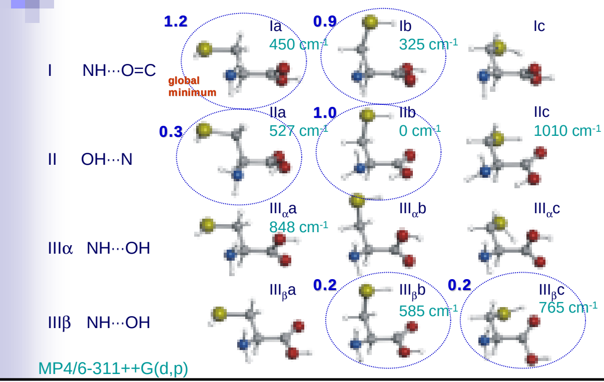

GABA (ácido γ-aminobutírico)

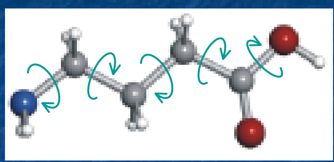

m.p. 195 C

One of the most important inhibitor neurotransmitters
High concentration in the Central Nervous System

GABA ✹ 324 conformers

GABA (ácido γ-aminobutírico)

Low energy conformers

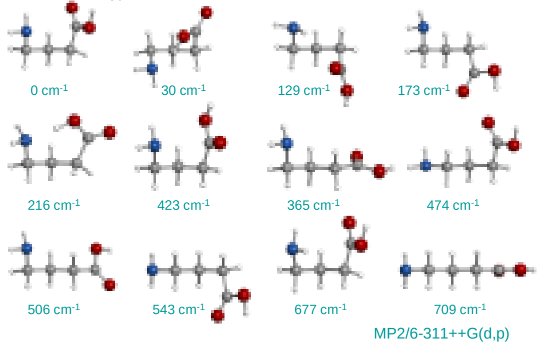

GABA (ácido γ-aminobutírico)

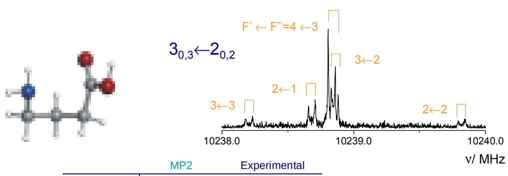

	MP2	Experimental
A / MHz	4129	4194.96418 (11)
B / MHz	1835	1792.83867 (40)
C / MHz	1670	1630.69973 (35)
Δ_J / kHz		1.3007 (84)
Δ_{JK} / kHz		3.80 (16)
Δ_K / kHz		9.14 (30)
δ_J / kHz		0.1020 (74)
δ_K / kHz		[0.0]
χ_{aa} / MHz	-2.64	-2.2733 (20)
χ_{bb} / MHz	2.61	2.5532 (30)
χ_{cc} / MHz	0.03	-0.2799 (70)
σ / kHz		2.8
N		54

GABA (ácido γ-aminobutírico)

intramolecular interactions

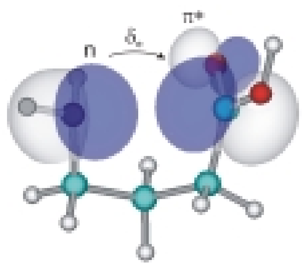

n ··· π* remote delocalization
Burgi-Dunitz trajectory

NBO analysis
RHF/6-311++G(d,p)
MP2/6-311++G(d,p)

Glycine···H_2O: Experimental set-up

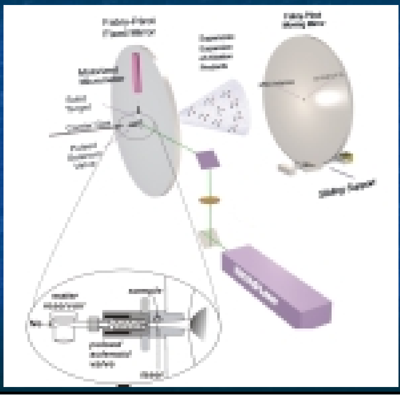

Glycine···H_2O: Rotational spectrum

	Parent
	Rotational cons
A (MHz)	8437.979 (149)
B (MHz)	1613.41327 (71)
C (MHz)	1378.06131 (51)
	Planar moment
P_c (u Å^2)	3.19871 (67)
	Centrif. Distort.
D_J (kHz)	0.4296 (59)
D_{JK} (kHz)	-1.359 (172)
D_K (kHz)	[0.0]
d_J (kHz)	0.1019 (61)
d_K (kHz)	[0.0]
	^{14}N NQC tensor
χ_{aa} (MHz)	-3.285 (27)
χ_{bb} (MHz)	1.694 (67)
χ_{cc} (MHz)	1.590 (67)
s (kHz)	3.1
N	30

Once the transitions from Glycine I and II were excluded

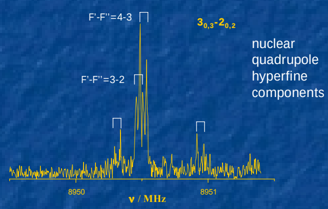

nuclear quadrupole hyperfine components

$$H = H_R^{(A)} + H_Q$$

Semirigid Rotor   Nuclear Quadrupole Term

Glycine···H_2O: Experiment vs. theory

Experiment

	Parent
	Rotational cons
A (MHz)	8437.979 (149)
B (MHz)	1613.41327 (71)
C (MHz)	1378.06131 (51)
	Planar moment
P_c (u Å^2)	3.19871 (67)
	Centrif. Distort.
D_J (kHz)	0.4296 (59)
D_{JK} (kHz)	-1.359 (172)
D_K (kHz)	[0.0]
d_J (kHz)	0.1019 (61)
d_K (kHz)	[0.0]
	^{14}N NQC tensor
c_{aa} (MHz)	-3.285 (27)
c_{bb} (MHz)	1.694 (67)
c_{cc} (MHz)	1.590 (67)
s (kHz)	3.1
N	30

MP2/6-311++G(d,p)

Conformer Ia	Conformer IIIa
Rotational constants	
8440	7978
1614	1654
1379	1404
Planar moment	
3.26	4.47
^{14}N quadrupole coupling tensor	
-3.57	-3.95
1.69	2.14
1.88	1.80
Relative energy (kJ mol^{-1})	
0.0	4.7

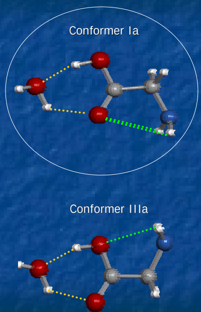

Glycine···H_2O: Isotopic species

	Parent	^{15}N-glycine ···H_2O	^{15}N-glycine ···$H_2{}^{18}O$
	Rotational constants		
A (MHz)	8437.979 (149)	8401.068 (109)	8374.89 (11)
B (MHz)	1613.41327 (71)	1579.66148 (61)	1500.69207 (52)
C (MHz)	1378.06131 (51)	1352.44092 (45)	1293.54511 (39)
	Planar moment		
P_c (u Å^2)	3.19871 (67)	3.20301 (51)	3.20776 (51)
	Centrifugal distortion constants		
D_J (kHz)	0.4296 (59)	0.3834 (55)	0.3634 (47)
D_{JK} (kHz)	-1.359 (172)	[0.0]	[0.0]
D_K (kHz)	[0.0]	[0.0]	[0.0]
d_J (kHz)	0.1019 (61)	0.0777 (56)	0.0613 (18)
d_K (kHz)	[0.0]	[0.0]	[0.0]
	^{14}N nuclear quadrupole coupling tensor		
c_{aa} (MHz)	-3.285 (27)		
c_{bb} (MHz)	1.694 (67)		
c_{cc} (MHz)	1.590 (67)		
s (kHz)	3.1	1.8	1.6
N [c]	30	11	11

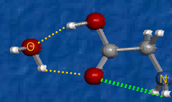

Glycine···H_2O: Structure

- Binding a single water molecule to Glycine proceeds through the carboxylic group and gives rise to a closed ring structure with two simultaneous intermolecular hydrogen bonds formed between the carbonyl group and one of the hydrogen atoms of water (O_w-H···O=C) and between the hydroxyl group and the electron lone pair at the oxygen atom of water (O_w···H-O-C).

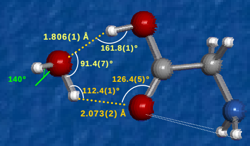

- The structure of Glycine-Water retains the preferred conformation I of the Glycine most stable form, with a *cis*-carboxylic group and a NH···O=C bifurcated intramolecular hydrogen bond

Microwave Spectroscopy:
Historical Overview

LASER ABLATION COMBINED WITH **MICROWAVE SPECTROSCOPY** IN A **SUPERSONIC JET** MAY CONSTITUTES A NEW TOOL WHICH CAN BE BROADLY APPLIED TO ROTATIONAL SPECTRA OF SOLIDS COMPOUNDS.

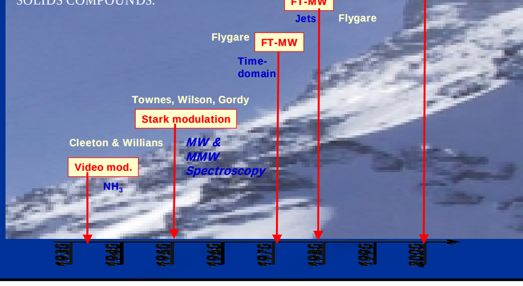

GRUPO DE ESPECTROSCOPIA MOLECULAR

Universidad de Valladolid

Funding:

- *Ministerio de Ciencia y Tecnología*
- *Junta de Castilla y León*